J. Electrochem. Sci. Eng. **00(0)** (2022) 000-000; http://dx.doi.org/10.5599/jese.1535

Open Access : : ISSN 1847-9286
www.jESE-online.org

Original scientific paper

Synthesis of ammonia from water and nitrogen using a composite cathode based on $La_{0.6}Ba_{0.4}Fe_{0.8}Cu_{0.2}O_{3-\delta}$-$Ce_{0.8}Gd_{0.18}Ca_{0.02}O_{2-\delta}$

Ibrahim A. Amar✉

Department of Chemistry, Faculty of Sciences, Sebha University, Sebha, Libya

Corresponding authorc: ✉ibr.amar@sebhau.edu.ly

Received: September 30, 2022; Accepted: November 5, 2022; Published: November 8, 2022

Abstract

Carbon-free electrochemical synthesis of ammonia is a promising technology for CO_2 emission reduction. This study aims to explore the electrocatalytic activity of A-site Ba-doped perovskite cathode catalyst ($La_{0.6}Ba_{0.4}Fe_{0.8}Cu_{0.2}O_{3-\delta}$, LBFCu) for ammonia synthesis from water and nitrogen. LBFCu was prepared via the sol-gel method using combined EDTA-citrate complexing agents and characterized by X-ray diffraction (XRD) and scanning electron microscope (SEM). Ammonia was successfully synthesised from water and nitrogen under atmospheric pressure, and LBFCu mixed with $Ce_{0.8}Gd_{0.18}Ca_{0.02}O_{2-\delta}$ (CGDC) was used as a cathode. When a voltage was applied to the cell containing CGDC-carbonate composite solid electrolyte, ammonia formation was observed at 375, 400, 425 and 450 °C. At 400 °C and 1.4 V, the maximum rate of ammonia production was achieved at 4.0×10^{-11} mol s^{-1} cm^{-2}, which corresponds to Faradaic efficiency of ~ 0.06 % at the current density of 19 mA cm^{-2}. According to the findings, the synthesis of ammonia directly from water and nitrogen may be considered a promising green synthesis technology.

Keywords

Ammonia production; electrosynthesis; electrocatalyst; perovskite oxide; oxide-carbonate composite electrolyte

Introduction

Ammonia is one of the most produced chemicals worldwide, widely used as a chemical feedstock for the production of reactive nitrogen compounds such as urea, ammonium nitrate, nitric acid, synthetic fibers, pharmaceuticals, resins, dyes, plastics and ammonium sulphate. The global production of ammonia reached ~160 million tons in 2019 [1,2]. Since its development in the early 1900s, the Haber-Bosch process has been applied for industrial production of ammonia, converting hydrogen and nitrogen gas into ammonia at high temperature (~500 °C) and high pressure (15 to 30 MPa), using fossil fuels (natural gases or coal) as energy sources, which now becomes a big challenge when moving toward renewable energy transition. The steam reforming step to generate hydrogen gas causes serious carbon emissions as it consumes approximately 84 % of the energy

required for the ammonia industry [3-6]. More than 300 million metric tons of CO_2 are generated per year from the ammonia production industry [7]. It is urgent to find an environmentally friendly process for the ammonia industry. Electrochemical synthesis of ammonia appears more and more attractive since renewable electricity is the energy source instead of fossil fuels [8-11]. Different catalysts have been developed for nitrogen reduction [12-15]. However, there are still challenges for the electrochemical process to be applied in the industry [16]. A number of review papers have been published to discuss the problems and strategies in the electrochemical synthesis of ammonia [15,17-19].

Solid-state electrochemical synthesis of ammonia has been reported [8,20-22]. H_2 was used as a precursor for ammonia synthesis in these reports, despite the problems associated with its production, purification, transportation and storage [6,23]. Ammonia synthesis directly from H_2O and N_2 will bypass the hydrogen production stage, which can help reduce the carbon emission in H_2 production when fossil fuel is used as energy resources [24]. It has been demonstrated that ammonia can be synthesised from H_2O and N_2 in electrolytic cells based on proton (H^+) or oxygen ion (O^{2-}) conducting electrolytes and different working electrodes (cathodes) [25-28]. The principle of the electrochemical synthesis of ammonia from H_2O and N_2 using oxygen-ion, and conducting electrolytes is presented in eqs. (1-3) [25].

At the cathode,

$$3H_2O + N_2 + 6e^- \rightarrow 3O^{2-} + 2NH_3 \quad (1)$$

At the anode, oxygen ions are converted to gaseous oxygen,

$$3O_2- \rightarrow 3/2O_2 + 6e^- \quad (2)$$

The overall reaction is:

$$3H_2O + N_2 \rightarrow {}^-2NH_3 + 3/2O_2 \quad (3)$$

Perovskite-type oxides are generally noted as ABO_3, where A is a rare-earth or alkaline earth element (*e.g*., La, Sr, Ba) and B is a transition metal element (*e.g.,* Fe, Cr, Co). These oxides are low-cost, easily synthesized, with high thermal stability and good catalytic activity [28-30]. Perovskite-based catalysts have been applied in solid oxide fuel cells (SOFCs) [31,32], solid oxide steam electrolysis cells (SOECs) [33,34], direct carbon fuel cells (DCFCs) [35], and electrochemical synthesis of ammonia [28,36-38].

In the literature, it has been reported that the catalytic activities of perovskite oxides were improved by the A-site doping strategy [39-41]. By A-site doping, oxygen vacancies will be generated [39]. It was also reported that oxygen vacancies at the cathode improve the catalytic activity of ammonia synthesis [42]. In the previous study [43], A-site Sr-doped perovskite cathode $La_{0.6}Sr_{0.4}Fe_{0.8}Cu_{0.2}O_{3-\delta}$ (LSFCu) was successfully employed for the electrochemical synthesis of ammonia from water and nitrogen.

Alkaline earth elements, such as barium, were found to be an efficient promoters for ammonia synthesis catalysts [44-47]. It was reported that Ba-promoted iron-cobalt alloys and Ba-promoted cobalt catalysts supported on magnesium-lanthanum mixed oxide catalysts showed significantly higher activity for ammonia synthesis [46,47]. Based on this discussion, it is anticipated that A-site Ba-substituted perovskite oxide with the form $La_{0.6}Ba_{0.4}Fe_{0.8}Cu_{0.2}O_{3-\delta}$ (LBFCu) may have good electrocatalytic activity for ammonia synthesis. To the best of our knowledge, the electrosynthesis of ammonia using LBFCu as an electrocatalyst (cathode) has not been reported yet. Thus, in this paper electrocatalyst activity of LBFCu for ammonia synthesis from water and nitrogen is explored.

Experimental

Materials synthesis

$La_{0.6}Ba_{0.4}Fe_{0.8}Cu_{0.2}O_{3-\delta}$ (LBFCu) was synthesised *via* a combined EDTA-citrate complexing sol-gel process [48]. Lanthanum oxide (La_2O_3, Alfa Aesar, 99 %), barium nitrate ($Ba(NO_3)_2$, Alfa Aesar, 99 %) ($Fe(NO_3)_3{\cdot}9H_2O$, Alfa Aesar, 98 %) and cobalt nitrate ($Co(NO_3)_2{\cdot}6H_2O$, Sigma Aldrich, 98 %) were used. La_2O_3 was dissolved in diluted nitric acid to form a lanthanum nitrate solution. Calculated amounts of $Ba(NO_3)_2$, $Fe(NO_3)_3{\cdot}9H_2O$ and $Co(NO_3)_2{\cdot}6H_2O$ were dissolved in deionised water, and then added to the lanthanum nitrate solution. Citric acid and EDTA (ethylene-diamine-tetra-acetic acid) were added as complexing agents, with a ratio of citric acid: EDTA: metal cations of 1.5:1:1. Dilute ammonia solution was added to adjust the pH to ~ 6. On a hot plate, water in the mixture was gradually vaporized under heating and stirring. The resultant powder was ground and subsequently calcined in air at 900 °C for 2 h, at 5 °C min^{-1} heating/cooling rate, to obtain single-phase LBFCu.

$Sm_{0.5}Sr_{0.5}CoO_{3-\delta}$ (SSCo) catalyst, and Gd and Ca co-doped ceria $Ce_{0.8}Gd_{0.18}Ca_{0.02}O_{2-\delta}$ (CGDC) powders were also synthesised *via* combined EDTA-citrate complexing sol-gel process. The composite electrolyte was prepared by mixing CGDC and ternary carbonate ($(Li/Na/K)_2CO_3$) at a weight ratio of 70:30, as described elsewhere [27].

Materials characterization

X-ray diffraction (XRD) data were collected at room temperature using a Panalytical X'Pert Pro diffractometer with Ni-filtered CuKα radiation (λ = 0.15405 nm), using 40 kV and 40 mA, fitted with a X'Celerator detector. Absolute scans were recorded in 2θ ranges 5-100°, at a step size of 0.0167°. The crystallite size (*D*) was estimated using Sherrer's equation as follows:

$$D = \frac{0.9\lambda}{\beta \cos\theta} \tag{4}$$

where λ is the X-ray wavelength, θ Bragg's diffraction angle and β is the full width at half maximum (FWHM).

The microstructures of the prepared catalyst and the cross-sectional area of the single cell were examined using a Hitachi SU6600 Scanning electron microscope (SEM).

Thermo-gravimetry and differential scanning calorimetry (TGA/DSC) analyses were performed using a Stanton Redcroft STA/TGH series STA 1500, operating through a Rheometric Scientific system interface controlled by the software RSI Orchestrator. The thermal behaviour of LBFCu ash was studied in flowing air at a flow rate of 50 ml min^{-1}. The thermal behaviour of LBFCu (cathode) was investigated in N_2 atmosphere from room temperature up to 500 °C at 10 °C min^{-1} heating/cooling rate.

Fabrication of the single cell for ammonia synthesis

A tri-layer single cell was fabricated through the one-step dry-pressing method. The anode consisted of SSCo, CGDC, and starch as a pore former, at a weight ratio of 61:26:13. The electrolyte was CGDC/$(Li/Na/K)_2CO_3$ (70 : 30 wt.%). The cathode consisted of LBFCu, CGDC and starch, with a weight ratio of 61:26:13. The anode, electrolyte and cathode were fed into the die, layer by layer, with the aid of a sieve to ensure uniform powder distribution, and then uniaxially pressed at 121 MPa. The freshly made pellet was sintered in air at 700 °C for 2 h, at 2 °C min^{-1} heating/cooling rate. The active surface area of the cathode was 0.785 cm^2. The silver paste was painted in a grid pattern on the electrode surface as a current collector. Ag wires were used as output terminals.

Ammonia synthesis

The fabricated cell was sealed into a self-designed double-chamber reactor using ceramic paste (Aremco, Ceramabond 552). The electrolytic cell was constructed: air, SSCo-CGDC | CGDC-carbonate | LBFCu-CGDC, 3 % H_2O-N_2. The cathode chamber was fed with 3 % H_2O-N_2 (BOC). The water vapour (3 % H_2O) was supplied to the cathode chamber by bubbling N_2 through liquid water at 25 °C. The anode was exposed to air. The voltage was applied by a Solartron 1287A electrochemical interface controlled by the software CorrWare/CorrView. A constant voltage was applied to the cell. Ammonia synthesised at the cathode chamber was absorbed in 20 mL diluted HCl (0.01 mol L^{-1}). The concentration of NH_4+ in the absorbed solution was analysed using ion selective electrode, ISE (Thermo Scientific Orion Star A214). The rate of ammonia formation and Faradaic efficiency were calculated as follows [49,50]:

$$r_{NH_3} = \frac{C_{NH_4^+} V}{M_{NH_4^+} tA} \quad (5)$$

$$\text{Faradaic efficiency} = \frac{3Fr_{NH_3}}{j} 100 \quad (6)$$

where r_{NH_3} is the rate of ammonia formation (mol s^{-1} cm^{-2}), $c_{NH_4^+}$ is the concentration of NH_4^+ (g mL^{-1}), V is the volume of HCl solution (20 mL), M_{NH4^+} is the molar mass NH_4^+ (18 g mol^{-1}), t / s is ammonia collection time, A is the cathode geometric surface area (0.785 cm^2), F is the Faradaic constant and j is the generated current density, mA cm^{-2}, (taking into consideration the cathode geometric surface area).

AC impedance spectroscopy (IS) measurements were performed using a Schlumberger Solartron SI 1250 analyser, coupled with a SI 1287 Electrochemical Interface controlled by Z-plot/Z-view software. The in-situ AC impedance spectra of the electrolytic cell under open circuit conditions were recorded with 100 mV AC excitation signal amplitude over the frequency range from 65 kHz to 0.01 Hz.

Results and discussion

Thermal and XRD analysis

Thermal analysis (TGA-DSC) of the corresponding ash indicates that the reaction completes at about 830 °C (Figure 1a), therefore 900 °C was chosen as a firing temperature for the preparation of $La_{0.6}Ba_{0.4}Fe_{0.8}Cu_{0.2}O_{3-\delta}$ (LBFCu). When the ash was calcined in air at 900 °C for 2 h, single-phase perovskite oxide $La_{0.6}Ba_{0.4}Fe_{0.8}Cu_{0.2}O_{3-\delta}$ was obtained, and its X-ray diffraction pattern shows a typical cubic perovskite oxide structure. Therefore, the space group Pm-3m (221) was used as the starting model for Rietveld refinement [51]. Wyckoff sites assigned to La (and Ba), Fe (and Cu) and O were 1a, 1b and 3d, respectively. Rietveld refinements were carried out using the General Structure Analysis System (GSAS) [52]. The experimental data, calculated profile and the difference between experimental and calculated profiles for $La_{0.6}Ba_{0.4}Fe_{0.8}Cu_{0.2}O_{3-\delta}$ are shown in Figure 2. The final refined structural data and thermal factors are listed in Table 1. The lattice parameters are given in Table 2. The crystallite size of LBFCu is 32.30 nm, as estimated from Sherrer's equation (4).

Figure 1b shows TGA-DSC curves of LBFCu in the N_2 atmosphere from room temperature up to 500 °C. From room temperature to 150 °C, weight losses of about 0.6 and 0.8 % were observed at 80 and 140 °C, corresponding to the likely losses of absorbed water and other gases. From 150 to 500 °C, a 1 % weight loss was observed, possibly due to the loss of lattice oxygen from the

$La_{0.6}Ba_{0.4}Fe_{0.8}Cu_{0.2}O_{3-\delta}$ structure. Figure 1b shows no obvious thermal effects in the DSC curve, indicating no phase transition or sample decomposition and no reaction between LBFCu and N_2 in the measured temperature range. Figure 2b is the XRD pattern of the LBFCu catalyst after thermal analysis in the N_2 atmosphere. $La_{0.6}Ba_{0.4}Fe_{0.8}Cu_{0.2}O_{3-\delta}$ retains the same perovskite structure, indicating its thermal stability in N_2. The refined lattice parameters are listed in Tables 1 and 2. After thermal measurements, cell volume expanded from 0.06066 (1) to 0.06094 (1) nm^3, indicating that the transition elements located at B-sites might have been slightly reduced.

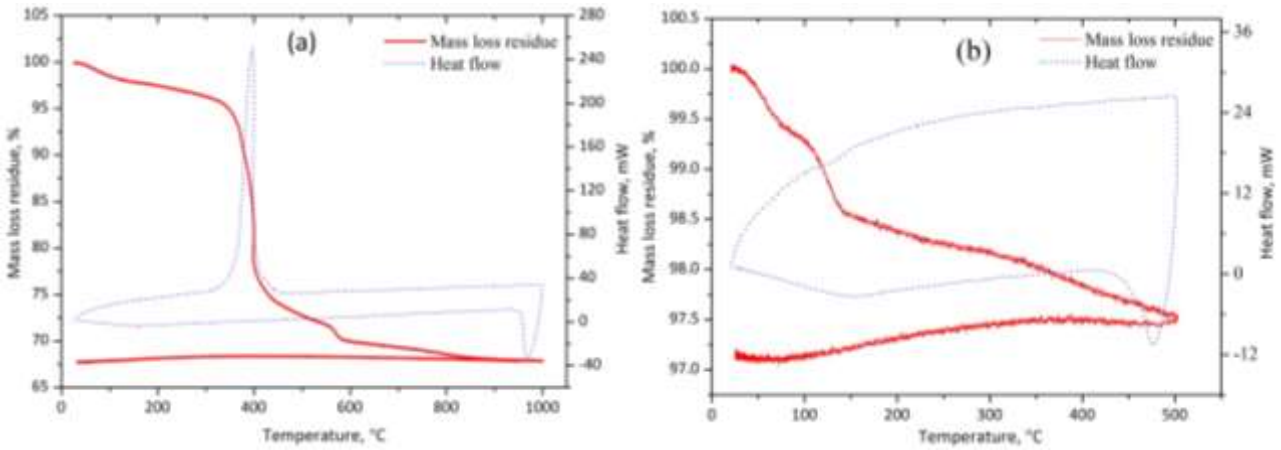

***Figure 1**. (a) TGA-DSC curves up to 500 °C of (a) LBFCu ash; (b) LBFCu catalyst in nitrogen*

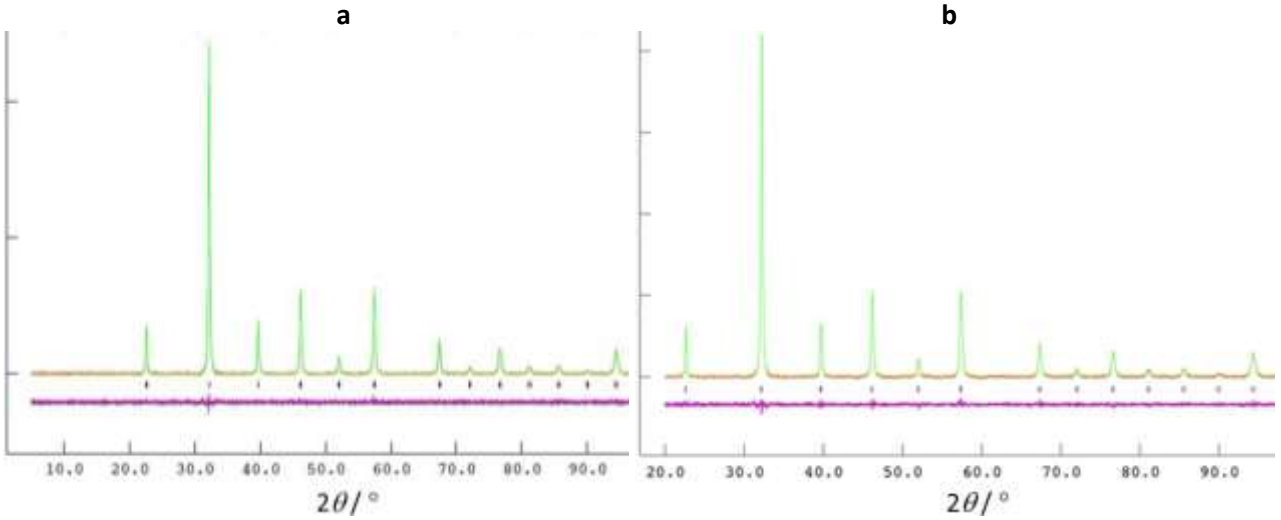

***Figure 2.** Rietveld refinement plot of the XRD data of A: LBFCu calcined in air at 900 °C for 2 h and B: LBFCu after STA analysis in N_2 at 500 °C. Experimental (red), calculated (green) and the difference between experimental and and calculated profiles (purple)*

***Table 1.** Atomic positions and thermal factors after refinement for $La_{0.6}Ba_{0.4}Fe_{0.8}Cu_{0.2}O_{3-\delta}$.*

Atom	*x*	*y*	*z*	Occupancy	$U_{iso} \times 100$	
					LBFCu ash[a]	LBFCu catalyst[b]
La	0	0	0	0.6	1.50 (1)	1.48 (1)
Ba	0	0	0	0.4	1.50 (1)	1.48 (1)
Fe	0.5	0.5	0.5	0.8	1.69 (1)	l.67 (1)
Cu	0.5	0.5	0.5	0.2	1.69 (1)	l.67 (1)
O	0.5	0.5	0	1	3.71 (1)	4.18 (1)

[a]LBFCu ash calcined in air at 900 °C for 2 h and [b]LBFCu catalyst after STA measurment in N_2 at 500 °C

Table 2. *Refinement parameters for $La_{0.6}Ba_{0.4}Fe_{0.8}Cu_{0.2}O_{3-\delta}$.*

Parameters	LBFCu ash fired in air at 900 °C for 2 h	LBFCu catalyst after STA analysis in N_2 at 500 °C
Crystal system	Cubic	Cubic
Space group	*Pm-3m* (221)	*Pm-3m* (221)
$a = b = c$ / nm	0.39292 (2)	0.39351
V / nm^3	0.06066 (1)	0.06094 (1)
ρ_{th} / g cm^{-3}	6.670	6.640
R_p / %	3.80	5.95
wR_p / %	4.96	7.76
χ^2	1.310	1.191

SEM analysis

Figure 3a shows the SEM image of LBFCu powder calcined in air at 900 °C for 2 h, showing a microporous structure with fine agglomerated particles of different sizes and shapes. Figure 3b is an SEM micrograph of the cross-sectional area of a single cell (before testing) sintered in air at 700 °C for 2 h. The cell consists of an SSCo-CGDC anode, CGDC-$(Li/Na/K)_2CO_3$ electrolyte and LBFCu-CGDC cathode. Figure 3b suggests a good adhesion between the dense electrolyte layer and both porous electrodes, indicating good contacts between them, and that CGDC-carbonate composite is compatible with both SSCo-CGDC and LBFCu-CGDC.

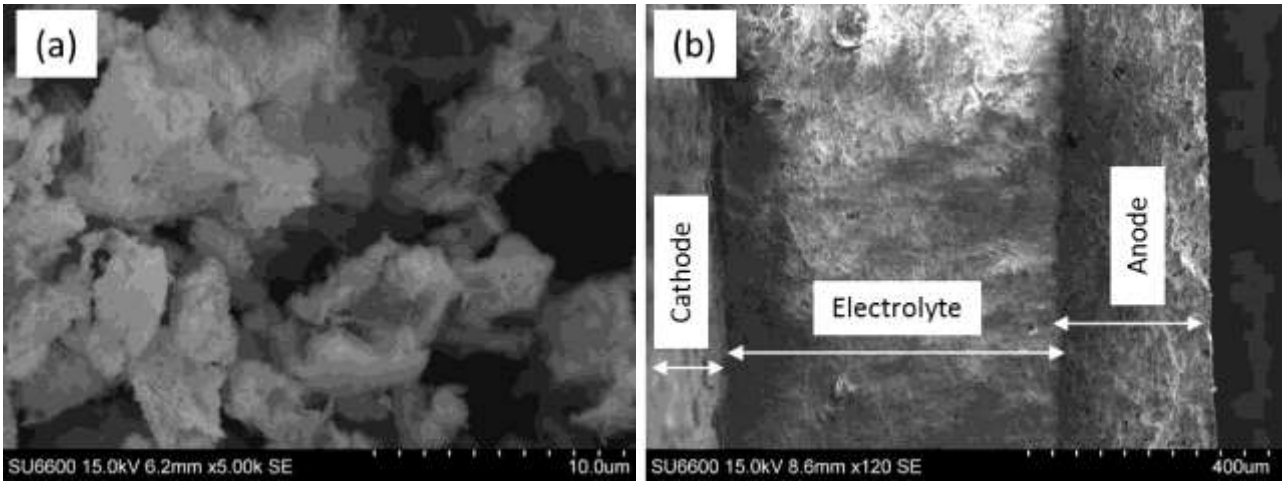

Figure 3. *SEM images of (a) LBFCu calcined in air at 900 °C; (b) cross-sectional area of the single cell before the ammonia synthesis*

Synthesis of ammonia at different temperatures

Figure 4 is the electrolytic cell performance during ammonia synthesis at 1.4 V over a period of 30 min operated at different temperatures (375-450 °C). The performance is stable under all operating temperatures. The current densities increase with the increase of operating temperature, a maximum value of about 33 mA cm^{-2} was achieved at 450 °C. The increase of current density at higher temperatures could be attributed to the increase of the ionic conductivity of electrolyte and the decrease of electrode polarisation resistance [20].

In-situ AC impedance spectra of the electrolytic cell under open circuit conditions at different temperatures (375-450 °C) are shown in Figure 5. The impedance spectra consist of one rather small and depressed semicircle at high frequencies and an almost straight line at low frequencies, suggesting at least two electrode processes. Figure 5 also shows that the ohmic resistance (R_{ohm}) of electrolyte, seen as the high-frequency intersection of the depressed semicircle with the real

impedance (Z') axis, decreased significantly with increased temperature and reached the lowest value of 5.86 Ω at 450 °C (inset of Figure 5). Another words, the ionic conductivity of the electrolyte increased at higher temperatures. When the cell operating temperature is increased, there was also a significant decrease in the polarisation resistance (R_p), seen as a diameter of a depressed semicircle, with the lowest value of 0.92 Ω attained at 450 °C, due to the higher activity of both composite electrodes (cathode and anode) at higher temperature [27].

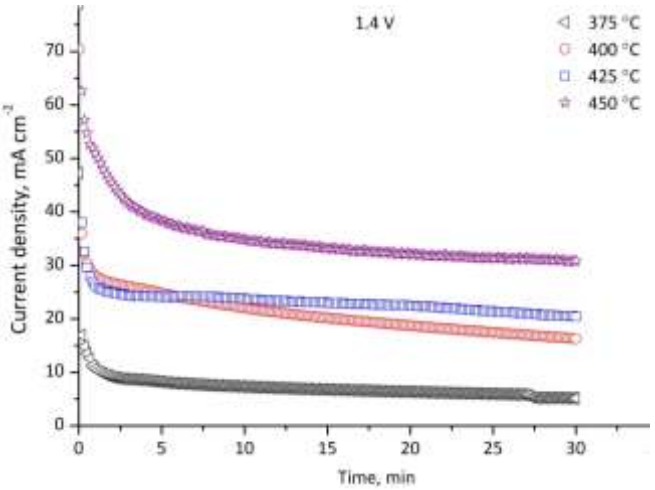

Figure 4. *Electrolytic cell performance stability at 1.4 V and 375-450 °C. The electrolytic cell: air, SSCo-CGDC|CGDC-carbonate|LBFCu-CGDC, 3% H_2O-N_2*

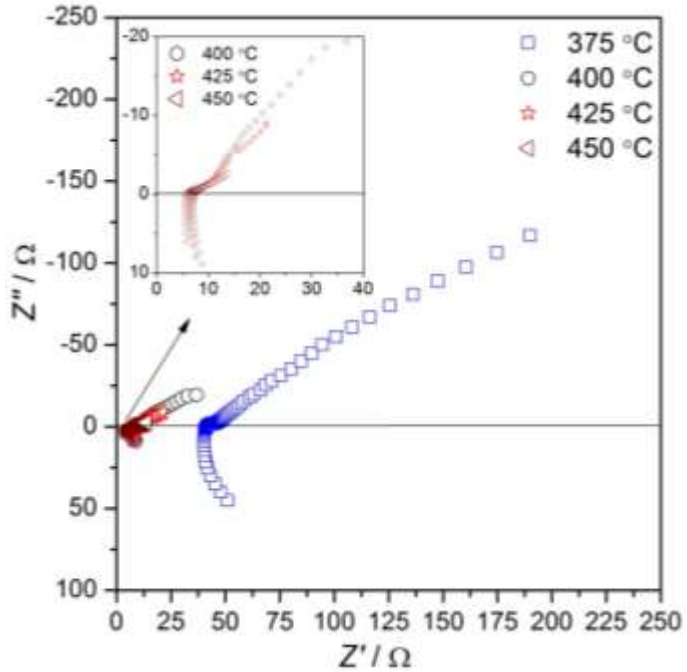

Figure 5. *Impedance spectra of the electrolytic cell containing LBFCu-CGDC cathode in CGDC-carbonate electrolyte, under open circuit conditions, at different temperatures (375-450 °C)*

The rate of ammonia formation was investigated at different temperatures from 375 to 450 °C, with a constant applied voltage of 1.4 V, as shown in Figure 6. The maximum ammonia formation rate of 4.0×10^{-11} mol s^{-1} cm^{-2} was obtained at 400 °C, with the generated current density of 19 mA cm^{-2} (Figure 4) and a Faraday efficiency of 0.06 % (Figure 6). This ammonia formation rate is comparable with that of A-site Sr-doped ($La_{0.6}Sr_{0.4}Fe_{0.8}Cu_{0.2}O_{3-\delta}$, LSFCu) perovskite cathode (5.0×10^{-11} mol s^{-1} cm^{-2} at 400 °C) [43]. This increase in the ammonia production rate from 375 to 400 °C could be ascribed to

the higher oxygen-ion conductivity of the composite electrolyte [20]. However, when the operating temperature was further increased, the ammonia formation decreased significantly and reached the lowest value at 450 °C. This could be attributed to ammonia decomposition at higher temperatures [21,27].

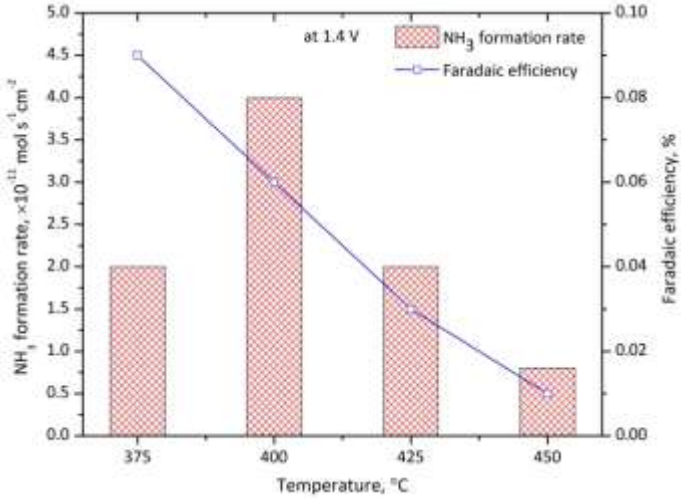

Figure 6. *Dependence of the rate of ammonia formation on the operating temperature*

Synthesis of ammonia at different applied voltages

To investigate the effect of the applied potential on the formation rate of ammonia, the cell operating temperature at a constant value (400 °C) and different voltage from 1.2 to 1.8 V was applied. Figure 7 shows the cell performance during 30 min of ammonia synthesis processes at different applied voltages (1.2-1.8 V) at 400 °C. The electrolytic cell performances were stable. The current density increased with increased applied voltage from 1.2 to 1.4 V, indicating that more oxygen ions were transported through the electrolyte to the anode. However, when the applied voltage was increased above 1.4 V, the current decreased, with the lowest value obtained at 1.8 V, which means the transportation of O^{2-} through the electrolyte to the anode becomes more and more difficult at voltages above 1.4 V. This could be explained by the blocking effect of Li^+, Na^+ and K^+ ions. Under the electric field, these positively charged ions will move and accumulate at the cathode/electrolyte interface to form a layer that will partially block the transfer of oxygen ions (O^{2-}) and result in lower current densities [27,53].

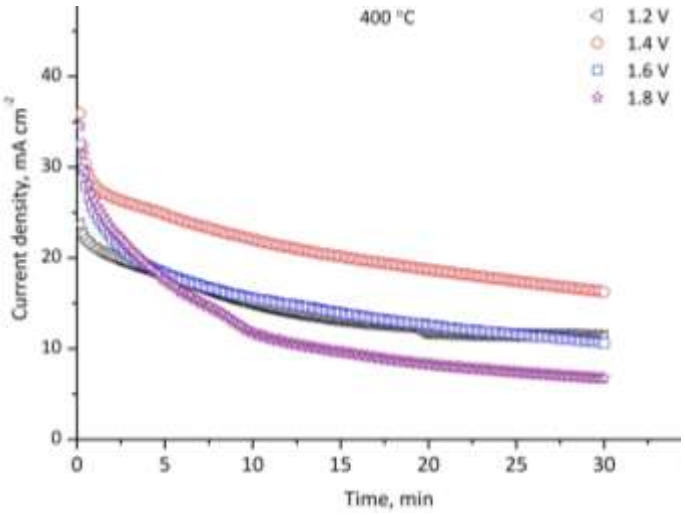

Figure 7*. Electrolytic cell performance stability at 400 °C and 1.2-1.8 V. The electrolytic cell: air, SSCo-CGDC|CGDC-carbonate|LBFCu-CGDC, 3% H_2O-N_2*

The formation rates of ammonia and Faradaic efficiency at different voltages are presented in Figure 8. The same trend for current densities was observed for formation rates and Faradaic efficiencies. From 1.2 to 1.4 V, the formation rate of ammonia increased with the increase of the applied voltage and reached a maximum value of 4.0×10^{-11} mol s^{-1} cm^{-2} at 1.4 V, with a corresponding current density of ~19 mA cm^{-2} and a Faradaic efficiency of 0.06 %. When the applied voltage was further increased above 1.4 V, the ammonia production rate decreased significantly and reached its lowest value of 1.0×10^{-11} mol s^{-1} cm^{-2} at 1.8 V, corresponding to a current density of 8.68 mA cm^{-2} and a Faradaic efficiency of 0.03 %. Low ammonia formation rates with corresponding low Faradaic efficiencies at higher voltages indicate that more than one process occurs at the cathode, and hydrogen evolution might be the predominant [26,49,54]. The formation rate of ammonia achieved using LBFCu is still higher than that reported using a Ru-based catalyst and water and nitrogen as precursors to synthesise ammonia (3.75×10^{-13} mol s^{-1} cm^{-2} at 650 °C) [25]. This could be due to the higher ionic conductivity of the CGDC-carbonate composite electrolyte compared to YSZ and the low operating temperature applied in that research (400 °C) that reduced associated ammonia decomposition.

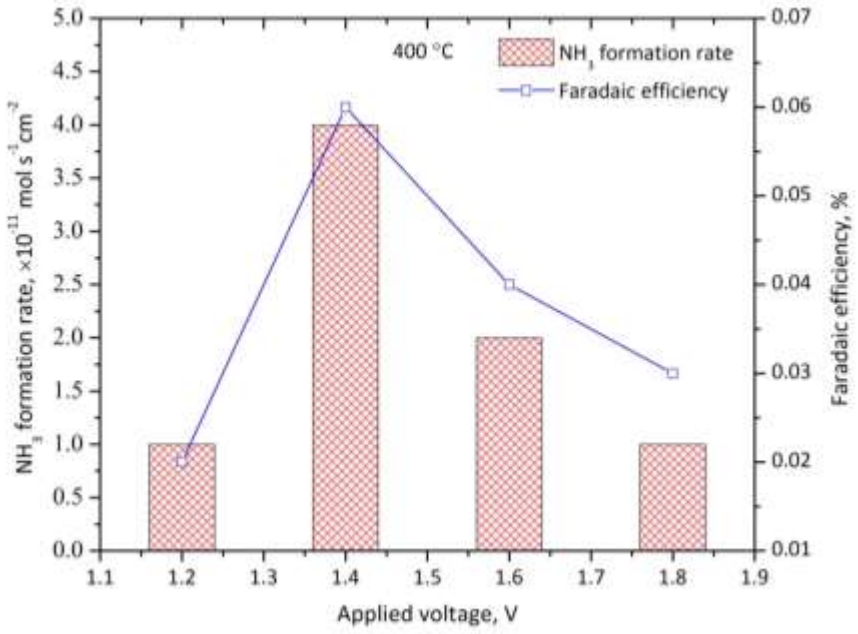

Figure 8. *Dependence of the rate of ammonia formation on the applied voltage at 400 °C*

Conclusions

In summary, the electrocatalytic activity of A-site Ba-substituted perovskite cathode ($La_{0.6}Ba_{0.4}Fe_{0.8}Cu_{0.2}O_{3-\delta}$, LBFCu) for ammonia synthesis from water and nitrogen was successfully explored. The XRD results demonstrated that a single-phase perovskite oxide (LBFCu) with a cubic structure was obtained. Ammonia was successfully synthesised from water and nitrogen under atmospheric pressure using LBFCu-$Ce_{0.8}Gd_{0.18}Ca_{0.02}O_{2-\delta}$ (CGDC) composite as a cathode, and CGDC-carbonate as composite solid electrolyte. The maximum rate of ammonia production was found to be 4.0×10^{-11} mol s^{-1} cm^{-2} at 400 °C and 1.4 V. The results indicated that a lower operating temperature is favourable to reducing ammonia decomposition, which at the same time, requests higher electrolyte conductivity and higher catalytic activity of the cathode. The results revealed that the catalytic activity of the proposed cathode catalyst (LBFCu) towards ammonia synthesis formation is comparable to that of A-site Sr-substituted perovskite cathode ($La_{0.6}Sr_{0.4}Fe_{0.8}Cu_{0.2}O_{3-\delta}$). According to

the findings, the prepared Ba-containing electrocatalyst (LBFCu) may be considered as a promising candidate material for carbon-free ammonia synthesis.

Acknowledgements: *The author would like to thank Professor Shanwen Tao from the University of Warwick in Coventry, UK, for providing the ammonia synthesis equipment. The author would also like to thank Dr. Rong Lan of Coventry University in Coventry, UK, for her assistance and encouragement. The authors would also like to thank Strathclyde University's Department of Pure and Applied Chemistry in Glasgow, UK, for the XRD and SEM analysis.*

Conflict of interest

Authors declare that there is no conflict of interest related to publishing of the present work.

References

[1] S. Ghavam, M. Vahdati, I. Wilson, P. Styring, Sustainable ammonia production processes, *Frontiers in Energy Research* **9** (2021) 580808. https://doi.org/10.3389/fenrg.2021.580808

[2] *Mineral Commodity Summaries 2020*, U.S. Geological Survey, 2020. p. 200. https://doi.org/10.3133/mcs2020

[3] M. Appl, *Ammonia: Principles and Industrial Practice,* Wiley-VCH, 1999. ISBN: 3527295933

[4] I. Rafiqul, C. Weber, B. Lehmann, A. Voss, Energy efficiency improvements in ammonia production-perspectives and uncertainties, *Energy* **30** (2005) 2487-2504. https://doi.org/10.1016/j.energy.2004.12.004

[5] R. Michalsky, P. H. Pfromm, Chromium as reactant for solar thermochemical synthesis of ammonia from steam, nitrogen, and biomass at atmospheric pressure, *Solar Energy* **85** (2011) 2642-2654. https://doi.org/10.1016/j.solener.2011.08.005

[6] C. Kurien, M. Mittal, Review on the production and utilization of green ammonia as an alternate fuel in dual-fuel compression ignition engines, *Energy Conversion and Management* **251** (2022) 114990. https://doi.org/10.1016/j.enconman.2021.114990

[7] Y. Tanabe, Y. Nishibayashi, Developing more sustainable processes for ammonia synthesis, *Coordination Chemistry Reviews* **257** (2013) 2551-2564. https://doi.org/10.1016/j.ccr.2013.02.010

[8] G. Marnellos, M. Stoukides, Ammonia synthesis at atmospheric pressure, *Science* **282** (1998) 98-100. https://doi.org/10.1126/science.282.5386.98

[9] I. A. Amar, R. Lan, C. T. G. Petit, S. Tao, Solid-state electrochemical synthesis of ammonia: a review, *Journal of Solid State Electrochemistry* **15** (2011) 1845-1860. https://doi.org/10.1007/s10008-011-1376-x

[10] S. Giddey, S. P. S. Badwal, A. Kulkarni, Review of electrochemical ammonia production technologies and materials, *International Journal of Hydrogen Energy* **38** (2013) 14576-14594. https://doi.org/10.1016/j.ijhydene.2013.09.054

[11] I. Garagounis, A. Vourros, D. Stoukides, D. Dasopoulos, M. Stoukides, Electrochemical synthesis of ammonia: Recent efforts and future outlook, *Membranes* **9** (2019) 112. https://doi.org/10.3390/membranes9090112

[12] C. Zhang, Z. Wang, J. Lei, L. Ma, B.I. Yakobson, J. M. Tour, Atomic molybdenum for synthesis of ammonia with 50 % faradic efficiency, *Small* **18** (2022) 2106327. https://doi.org/10.1002/smll.202106327

[13] J. Xia, H. Guo, M. Cheng, C. Chen, M. Wang, Y. Xiang, T. Li, E. Traversa, Electrospun zirconia nanofibers for enhancing the electrochemical synthesis of ammonia by artificial nitrogen fixation, *Journal of Materials Chemistry A* **9** (2021) 2145-2151. https://doi.org/10.1039/d0ta08089f

[14] S. Ye, Z. Chen, G. Zhang, W. Chen, C. Peng, X. Yang, L. Zheng, Y. Li, X. Ren, H. Cao, D. Xue, J. Qiu, Q. Zhang, J. Liu, Elucidating the activity, mechanism and application of selective electrosynthesis of ammonia from nitrate on cobalt phosphide, *Energy & Environmental Science* **15** (2022) 760-770. https://doi.org/10.1039/d1ee03097c

[15] V. C. D. Graça, F. J. A. Loureiro, L. I. V. Holz, S. M. Mikhalev, A. J. M. Araújo, D. P. Fagg, Electrochemical ammonia synthesis: Mechanism, recent developments, and challenges in catalyst design*, Heterogeneous Catalysis* (2022) 497-514. https://doi.org/10.1016/B978-0-323-85612-6.00018-8

[16] T. Wu, W. Fan, Y. Zhang, F. Zhang, Electrochemical synthesis of ammonia: Progress and challenges, *Materials Today Physics* **16** (2021) 100310. https://doi.org/10.1016/j.mtphys.2020.100310

[17] G. Soloveichik, Electrochemical synthesis of ammonia as a potential alternative to the Haber–Bosch process, *Nature Catalysis* **2** (2019) 377-380. https://doi.org/10.1038/s41929-019-0280-0

[18] J. Yang, W. Weng, W. Xiao, Electrochemical synthesis of ammonia in molten salts, *Journal of Energy Chemistry* **43** (2020) 195-207. https://doi.org/10.1016/j.jechem.2019.09.006

[19] Y. Yao, J. Wang, U.B. Shahid, M. Gu, H. Wang, H. Li, M. Shao, Electrochemical synthesis of ammonia from nitrogen under mild conditions: Current status and challenges, *Electrochemical Energy Reviews* **3** (2020) 239-270. https://doi.org/10.1007/s41918-019-00061-3

[20] I. A. Amar, R. Lan, C. T. G. Petit, S. Tao, Electrochemical synthesis of ammonia aased on Co_3Mo_3N catalyst and $LiAlO_2$-$(Li,Na,K)_2CO_3$ composite electrolyte, *Electrocatalysis* **6** (2015) 286-294. https://doi.org/10.1007/s12678-014-0242-x

[21] W. B. Wang, X. B. Cao, W. J. Gao, F. Zhang, H. T. Wang, G. L. Ma, Ammonia synthesis at atmospheric pressure using a reactor with thin solid electrolyte $BaCe_{0.85}Y_{0.15}O_{3-\alpha}$ membrane, *Journal of Membrane Science* **360** (2010) 397-403. https://doi.org/10.1016/j.memsci.2010.05.038

[22] E. Vasileiou, V. Kyriakou, I. Garagounis, A. Vourros, A. Manerbino, W. G. Coors, M. Stoukides, Electrochemical enhancement of ammonia synthesis in a $BaZr_{0.7}Ce_{0.2}Y_{0.1}O_{2.9}$ solid electrolyte cell, *Solid State Ionics* **288** (2016) 357-362. https://doi.org/10.1016/j.ssi.2015.12.022

[23] S. Dutta, A review on production, storage of hydrogen and its utilization as an energy resource, *Journal of Industrial and Engineering Chemistry* **20** (2014) 1148-1156. https://doi.org/10.1016/j.jiec.2013.07.037

[24] T. Murakami, T. Nohira, T. Goto, Y. H. Ogata, Y. Ito, Electrolytic ammonia synthesis from water and nitrogen gas in molten salt under atmospheric pressure, *Electrochimica Acta* **50** (2005) 5423-5426. https://doi.org/10.1016/j.electacta.2005.03.023

[25] A. Skodra, M. Stoukides, Electrocatalytic synthesis of ammonia from steam and nitrogen at atmospheric pressure, *Solid State Ionics* **180** (2009) 1332-1336. https://doi.org/10.1016/j.ssi.2009.08.001

[26] I. A. Amar, M. M. Ahwidi, Electrocatalytic activity of $CoFe_{1.9}Mo_{0.1}O_4$-$Ce_{0.8}Gd_{0.18}Ca_{0.02}O_{2-\delta}$ composite cathode for ammonia synthesis from water and nitrogen, *World Journal of Engineering* **18** (2021) 490-496. https://doi.org/10.1108/wje-07-2020-0270

[27] I. A. Amar, C. T. G. Petit, G. Mann, R. Lan, P. J. Skabara, S. W. Tao, Electrochemical synthesis of ammonia from N_2 and H_2O based on $(Li,Na,K)_2CO_3$-$Ce_{0.8}Gd_{0.18}Ca_{0.02}O_{2-\delta}$ composite electrolyte and $CoFe_2O_4$ cathode, *International Journal of Hydrogen Energy* **39** (2014) 4322-4330. https://doi.org/10.1016/j.ijhydene.2013.12.177

[28] D. S. Yun, J. H. Joo, J. H. Yu, H. C. Yoon, J. N. Kim, C. Y. Yoo, Electrochemical ammonia synthesis from steam and nitrogen using proton conducting yttrium doped barium zirconate electrolyte with silver, platinum, and lanthanum strontium cobalt ferrite electrocatalyst, *Journal of Power Sources* **284** (2015) 245-251. https://doi.org/10.1016/j.jpowsour.2015.03.002

[29] G. Pecchi, M. Jiliberto, E. Delgado, L. Cadús, J. Fierro, Effect of B-site cation on the catalytic activity of $La_{1-x}Ca_xBO_3$ (B= Fe, Ni) perovskite-type oxides for toluene combustion, *Journal of Chemical Technology and Biotechnology* **86** (2011) 1067-1073. https://doi.org/10.1002/jctb.2611

[30] S. Zhang, G. Duan, L. Qiao, Y. Tang, Y. Chen, Y. Sun, P. Wan, S. Zhang, Electrochemical ammonia synthesis from N_2 and H_2O catalyzed by doped $LaFeO_3$ perovskite under mild conditions, *Industrial and Engineering Chemistry Research* **58** (2019) 8935-8939. https://doi.org/10.1021/acs.iecr.9b00833

[31] Z. Shao, S. M. Haile, A high-performance cathode for the next generation of solid-oxide fuel cells, *Nature* **431** (2004) 170-173. https://doi.org/10.1038/nature02863

[32] S. Presto, A. Barbucci, M. P. Carpanese, F. Han, R. Costa, M. Viviani, Application of La-doped $SrTiO_3$ in advanced metal-supported solid oxide fuel cells, *Crystals* **8** (2018) 134. https://doi.org/https://doi.org/10.3390/cryst8030134

[33] X. Yue, J. T. S. Irvine, $(La,Sr)(Cr,Mn)O_3$/GDC cathode for high temperature steam electrolysis and steam-carbon dioxide co-electrolysis, *Solid State Ionics* **225** (2012) 131-135. https://doi.org/10.1016/j.ssi.2012.06.015

[34] Y. Gan, J. Zhang, Y. Li, S. Li, K. Xie, J. T. S. Irvine, Composite oxygen electrode based on LSCM for steam electrolysis in a proton conducting solid oxide electrolyzer, *Journal of The Electrochemical Society* **159** (2012) F763-F767. https://doi.org/10.1149/2.018212jes

[35] W. Cai, D. Cao, M. Zhou, X. Yan, Y. Li, Z. Wu, S. Lü, C. Mao, Y. Xie, C. Zhao, J. Yu, M. Ni, J. Liu, H. Wang, Sulfur-tolerant Fe-doped $La_{0.3}Sr_{0.7}TiO_3$ perovskite as anode of direct carbon solid oxide fuel cells, *Energy* **211** (2020) 118958. https://doi.org/10.1016/j.energy.2020.118958

[36] F. Kosaka, N. Noda, T. Nakamura, J. Otomo, In situ formation of Ru nanoparticles on $La_{1-x}Sr_xTiO_3$-based mixed conducting electrodes and their application in electrochemical synthesis of ammonia using a proton-conducting solid electrolyte, *Journal of Materials Science* **52** (2017) 2825-2835. https://doi.org/10.1007/s10853-016-0573-5

[37] I. A. Amar, R. Lan, S. Tao, Synthesis of ammonia directly from wet nitrogen using a redox stable $La_{0.75}Sr_{0.25}Cr_{0.5}Fe_{0.5}O_{3-\delta}$-$Ce_{0.8}Gd_{0.18}Ca_{0.02}O_{2-\delta}$ composite cathode, *RSC Advances* **5** (2015) 38977-38983. https://doi.org/10.1039/c5ra00600g

[38] G. Xu, R. Liu, J. Wang, Electrochemical synthesis of ammonia using a cell with a Nafion membrane and $SmFe_{0.7}Cu_{0.3-x}Ni_xO_3$ (x = 0-0.3) cathode at atmospheric pressure and lower temperature, *Science in China Series B* **52** (2009) 1171-1175. https://doi.org/10.1007/s11426-009-0135-7

[39] K. Akinlolu, B. Omolara, O. Kehinde, T. Shailendra, Synthesis and characterization of A site doped lanthanum based perovskite catalyst for the oxidation of soot, *IOP Conference Series: Materials Science and Engineering* **509** (2019) 012062. https://doi.org/10.1088/1757-899x/509/1/012062

[40] Z. Dong, T. Xia, Q. Li, J. Wang, S. Li, L. Sun, L. Huo, H. Zhao, Addressing the origin of highly catalytic activity of A-site Sr-doped perovskite cathodes for intermediate-temperature solid oxide fuel cells, *Electrochemistry Communications* **140** (2022) 107341. https://doi.org/10.1016/j.elecom.2022.107341

[41] J. A. Onrubia-Calvo, B. Pereda-Ayo, I. Cabrejas, U. De-La-Torre, J. R. González-Velasco, Ba-doped vs. Sr-doped $LaCoO_3$ perovskites as base catalyst in diesel exhaust purification, *Molecular Catalysis* **488** (2020) 110913. https://doi.org/10.1016/j.mcat.2020.110913

[42] I. A. Amar, R. Lan, J. Humphreys, S. Tao, Electrochemical synthesis of ammonia from wet nitrogen via a dual-chamber reactor using $La_{0.6}Sr_{0.4}Co_{0.2}Fe_{0.8}O_{3-\delta}$-$Ce_{0.8}Gd_{0.18}Ca_{0.02}O_{2-\delta}$ composite cathode, *Catalysis Today* **286** (2017) 51-56. https://doi.org/10.1016/j.cattod.2016.09.006

[43] I. A. Amar, R. Lan, S. Tao, Electrochemical synthesis of ammonia directly from wet N_2 using $La_{0.6}Sr_{0.4}Fe_{0.8}Cu_{0.2}O_{3-\delta}$-$Ce_{0.8}Gd_{0.18}Ca_{0.02}O_{2-\delta}$ composite catalyst, *Journal of The Electrochemical Society* **161** (2014) H350-H354. https://doi.org/10.1149/2.021406jes

[44] W. Raróg-Pilecka, E. Miśkiewicz, L. Kępiński, Z. Kaszkur, K. Kielar, Z. Kowalczyk, Ammonia synthesis over barium-promoted cobalt catalysts supported on graphitised carbon, *Journal of Catalysis* **249** (2007) 24-33. https://doi.org/10.1016/j.jcat.2007.03.023

[45] E. Truszkiewicz, W. Raróg-Pilecka, K. Schmidt-Szałowski, S. Jodzis, E. Wilczkowska, D. Łomot, Z. Kaszkur, Z. Karpiński, Z. Kowalczyk, Barium-promoted Ru/carbon catalyst for ammonia synthesis: State of the system when operating, *Journal of Catalysis* **265** (2009) 181-190. https://doi.org/10.1016/j.jcat.2009.04.024

[46] H. Ronduda, M. Zybert, W. Patkowski, A. Ostrowski, P. Jodłowski, D. Szymański, L. Kępiński, W. Raróg-Pilecka, A high performance barium-promoted cobalt catalyst supported on magnesium–lanthanum mixed oxide for ammonia synthesis, *RSC Advances* **11** (2021) 14218-14228. https://doi.org/10.1039/d1ra01584b

[47] S. Hagen, R. Barfod, R. Fehrmann, C.J.H. Jacobsen, H.T. Teunissen, I. Chorkendorff, Ammonia synthesis with barium-promoted iron–cobalt alloys supported on carbon, *Journal of Catalysis* **214** (2003) 327-335. https://doi.org/10.1016/S0021-9517(02)00182-3

[48] Y. Ling, J. Yu, B. Lin, X. Zhang, L. Zhao, X. Liu, A cobalt-free $Sm_{0.5}Sr_{0.5}Fe_{0.8}Cu_{0.2}O_{3-\delta}$-$Ce_{0.8}Sm_{0.2}O_{2-\delta}$ composite cathode for proton-conducting solid oxide fuel cells, *Journal of Power Sources* **196** (2011) 2631-2634. https://doi.org/10.1016/j.jpowsour.2010.11.017

[49] H. Kim, Y.S. Chung, T. Kim, H. Yoon, J. G. Sung, H. K. Jung, W. B. Kim, L. B. Sammes, J. S. Chung, Ru-doped barium strontium titanates of the cathode for the electrochemical synthesis of ammonia, *Solid State Ionics* **339** (2019) 115010. https://doi.org/10.1016/j.ssi.2019.115010

[50] L. Qiao, G. Duan, S. Zhang, Y. Ren, Y. Sun, Y. Tang, P. Wan, R. Pang, Y. Chen, A.G. Russell, M. Fan, Electrochemical ammonia synthesis catalyzed with a CoFe layered double hydroxide – A new initiative in clean fuel synthesis, *Journal of Cleaner Production* **250** (2020) 119525. https://doi.org/10.1016/j.jclepro.2019.119525

[51] R. Genouel, C. Michel, N. Nguyen, F. Studer, M. Hervieu, B. Raveau, On the cubic perovskites $La_{0.2}Sr_{0.8}Cu_{0.4}M_{0.6}O_{3-y}$ (M = Co, Fe), *Journal of Solid State Chemistry* **119** (1995) 260-270. https://doi.org/10.1016/0022-4596(95)80040-V

[52] A. C. Larson, R.B . Von Dreele, General structure analysis system (GSAS)(Report LAUR 86-748), Los Alamos, New Mexico: Los Alamos National Laboratory, 2004.

[53] R. Lan, S. Tao, Electrochemical synthesis of ammonia directly from air and water using a $Li^+/H^+/NH_4^+$ mixed conducting electrolyte, *RSC Advances* **3** (2013) 18016-18021. https://doi.org/10.1039/C3RA43432J

[54] V. Kordali, G. Kyriacou, C. Lambrou, Electrochemical synthesis of ammonia at atmospheric pressure and low temperature in a solid polymer electrolyte cell, *Chemical Communications* (2000) 1673-1674. https://doi.org/10.1039/b004885m